

# Coronal mass ejection and solar activity for cycle 23 and 24; a comparative analysis of observational parameters

## Abstract

We analyzed sunspot tracers [sunspot number (SSN) and sunspot area (SSA)] and Coronal Mass Ejection (CME) observed parameters for cycle 23 and 24, comparing sunspot tracers time series with time series for CME parameters [Initial speed and Acceleration] for All and segregated CMEs for possible similarities in their variation pattern. A comparison of CME time series with solar activity (especially SSAT and SSN which seem to reflect the true general activity cycle) shows that fast CMEs follow the solar activity cycle but slow CMEs don't. Also, CMEs with positive and negative acceleration follow the solar cycle but lags behind by 3 months for cycle 24. However, the CME acceleration does not follow the solar cycle. CME distribution shows that Slow CMEs increase in initial speed from one cycle to the other with a corresponding decrease in acceleration for CMEs with fast speeds. There is an almost insignificant increase in acceleration for CMEs with positive and negative acceleration. These changes are perhaps due to effect of solar wind.

**Keywords:** Sunspot Number, CME, Solar Cycle

Volume 6 Issue 2 - 2022

**Umuogbana AO, Onuchukwu CC**

Department of Industrial Physics, Chukwuemeka Odumegwu Ojukwu University Uli, Nigeria

**Correspondence:** Umuogbana AO, Department of Industrial Physics, Chukwuemeka Odumegwu Ojukwu University Uli, 54 Egbu Road, Anambra State, Nigeria, Email laugojr@yahoo.com

**Received:** June 04, 2022 | **Published:** June 24, 2022

## Introduction

Coronal Mass Ejections (CMEs) are the most energetic phenomenon in the solar atmosphere. It represents the conversion of magnetic energy in the sun to plasma kinetic energy and flare thermal energy. CME is a transient phenomenon which differs from the quasi-steady plasma flow of solar wind. While CMEs are ejected into the solar wind, they often produce fast-mode MHD shocks, which in turn accelerate charged particles to very high energies. CMEs have great impact on planetary atmospheres an even terminal shocks of the heliosphere as it propagates into the interplanetary (IT) medium. The two major causes of solar variability are: solar evolution and magnetic field of the sun. The former is driven by conditions in the sun's core while the later is generated by a dynamo located at the bottom of the convection zone. The strength and structure of the resulting magnetic field is determined by differential rotation of sun and the turbulent convection at and below the surface. The differential rotation produces a mainly toroidal field near the base of the convection zone. Eventually, the strength of the field increases. Above a certain critical strength the field becomes unstable and individual loops start to rise towards the solar surface which they finally reach and pass through making them now accessible for observation. It's the interaction of this magnetic with convection that leads to the concentration of the field in filaments or bundle of filament called the flux tubes. The largest of these, the sunspots, have diameter similar to that of the earth and are visible as dark features on the solar surface. Whereas most of the magnetic field lines piercing the solar surface form loops and head back to the sun (they form closed magnetic flux), a small fraction is carried out by the solar wind into interplanetary space (called open magnetic flux). In particular, the closed magnetic flux field gives rise to a large number of phenomenon including Sunspots and Coronal Mass Ejection. The solar magnetic field, and hence also the associated activity cycle with a period of roughly 11 years. The Sunspots record and other often more indirect, proxies of solar magnetism have invited comparison.

## Data

CME Data was obtained by the current Large Angle and Spectrometric Coronagraph (LASCO) on board the solar and Hemisphere observatory (SOHO). From which the data is available at <http://cdaw.gsfc.nasa.gov/CME-list>. The collected data were not without gaps. These gaps occurred in

- June 24, 1998 – October 22, 1998
- Failure of all three gyroscopes caused an interruption from December 21, 1998 – February by 1999.
- In June 2003, the problem was overcome and nominal observation remained on July 10.
- The observed CME parameters selected from the catalogue are Initial Speed (IS) in km/s, acceleration in km/s<sup>2</sup>, and calculated force in N.

Solar cycle 23 spans August, 1996 – March, 2008 while solar cycle 24 spans December, 2008 – December 2019. I selected the CME data spanning from January, 1996 to May, 2020 (this included the ending of the solar cycle 22 and the beginning of solar cycle 25). There are about 13000 CMEs and 18000 CMEs for cycle 23 and cycle 24 respectively.

The data for the sunspot number and sunspot area for the years 1992 to 2019 were extracted from the OMNI web service archive of the NASA space physics data facility using the total monthly sunspot number and the monthly sunspot area. The monthly data with the sunspot area (for the Northern Hemisphere, Southern Hemisphere and the total solar surfaces) were extracted for cycle 23 and 24.

## Analysis and result

We present the monthly mean and median of CME parameters for cycle 23 and 24, and some selected outliers as in (a) The monthly total sunspot number (SSN) for cycle 23, the sunspot area (Northern

Hemisphere (SSANH) and Southern Hemisphere (SSASH)) and the total sunspot area (SSAT) estimated by summing the sunspot areas in both hemisphere. For the data for CME parameters, we started by debugging, so as to free data from any symbol that may affect analyses. Then

- A. We calculated the daily average, then weekly average and eventually monthly average, for ALL CMEs
- B. Then, (a) was performed on the following segregated CMEs
  - (i) Wide [ $> 1200$ ], normal [ $>500<1200$ ], narrow  $\leq 30^\circ$ .<sup>1</sup>
  - (ii) Slow [ $\leq 400\text{km/s}$ ], fast [ $>400\text{km/s}$ ] for linear speed.<sup>2</sup>
  - (iii) CME with positive and negative acceleration.<sup>3</sup>

Solar cycle 23 spans August, 1996 – March, 2008 while solar cycle 24 spans December, 2008 – December 2019. I selected the CME data spanning from January, 1996 to May, 2020 (this included the ending of the solar cycle 22 and the beginning of solar cycle 25). There are about 13000 CMES and 18000 CMES for cycle 23 and cycle 24 respectively.

The data for the sunspot number and sunspot area for the years 1992 to 2019 were extracted from the OMNI web service achieve of the NASA space physics data facility using the total monthly sunspot number and the monthly sunspot area. The monthly data with the sunspot area (for the Northern Hemisphere, Southern Hemisphere and the total solar surfaces) were extracted for cycle 23 and 24.

In Figure 1 We show the monthly total sunspot number (SSN), the sunspot area for the northern hemisphere (SSANH), Southern Hemisphere (SSASH), and the total sunspot area (SSAT) estimated by summing the sunspot areas in both southern and northern hemisphere. The tracers of solar activity all show a double-hump structure as reported by Ramesh and Kilcik; with SSN showing least in variations. The double-peak structure is due to the existence of two surges of toroidal fields<sup>4</sup> SSANH, SSASH, SSAT and SSN shows an almost exactly same trend with SSN and SSAT with exactly same behavior for cycle 23; noticeable is a general drip just before April 2001 but for cycle 24 the trends are not exactly as it is for cycle 23; SSAT and SSAH shows similar trend while SSNH different between April 2012 and December 2014. SSN for cycle 24 differs very much in trend to other sunspot tracers except from December 2014 to the end of the cycle for which trend is similar to other sunspot tracers. SSN for cycle 24 shows a much weaker cycle compared to cycle 23. SSN coincided with SSAT in cycle 23 (behaved exactly the same). SSN for cycle 24 shows much reduced Sunspot number compared to cycle 23.

### Analysis for Initial Speed (IS)

Coronagraph obtain images with a present time cadence and when CME occurs, the leading edge moves to a greater heliocentric distance. On measuring the heliospheric distance of the leading edge of a CME in each LASCO image, one obtains CME height as a function of time. Height-time measurements are made in the sky-plane, so all the derived parameters such as speed etc are the lower limits to the values. The height-time plots are then filtered to first order polynomial which gives an average speed within the LASCO field of view. The CME velocity generally means the radical projection speed of the top part of CME frontal loop. Fast CMEs for cycle 23 and fast 24 rises and then drops but slow CMEs for cycle 23 and 24 slightly rises; this implies that fast CMEs here show a more parabolic curve fast CMEs follow the sunspot cycle which lags it behind by 3 months, however, slow CMEs does not follow sunspot cycle (Figure 2). CMEs with positive acceleration and negative acceleration for cycles 23 shows a more

parabolic curve compared to its counterparts in cycle 24 respectively. It follows the solar cycle though lags it behind by 3 months for cycle 24 (Figure 3).

Distribution is skewed to the right with cycle 23 having 12485 number of CME events while cycle 24 has 17836. For slow CMEs, cycle 23 and 24 has 7872 and 11,190 CMEs respectively. Here, slow CMEs shows a more Gaussian distribution compared to the rest which are more or less right skewed. Peak values for slow CME 250km/s for both cycles. Average initial value for cycle 23 and 24 are 250 & 241 respectively. Distribution range is 0-550km/s (Figure 4).

For fast CMEs the number of CMEs are 5700 and 4284 for cycle 23 and 24. Peak value for fast CME are 760 and 680km/s respectively. Initial speed range is 200-2200km/s (Figure 5). For positive acceleration, cycle 23 and 24 has 6139 and 6028 CME events. Peak initial value for CME with positive acceleration is 200km/s for both cycles. Average initial speed values are 346 and 280km/s. The speed range is 0 – 1200km/s (Figure 6). Peak value for CME with negative acceleration is 400km/s for both cycles. Average speed range is 650 and 551km/s for cycle 23 and 24 respectively. Speed range is 200-2000km/s (Figure 7).

### Analysis for acceleration

Both cycle maintained an almost horizontal trend; with most of the peaks for cycle 23 happening between Jan, 2004 to Oct. 2006.

Acceleration is linear for both slow and fast CME. Corresponding cycles seems to overlap and of nearly same behavior except for few peaks and troughs; most prominent is the peaked oscillations at both ends of the time series for fast 24. They do not follow the solar cycle (Figure 8). PA 23 is a rising time series and NA 23, for the most part, is a reflection of it. PA 24 shows a slightly parabolic trend which is a reflection of NA 24. They do not follow the solar cycle (Figure 9). The CME mas is determined by measuring the number of electrons required in the plane of the sky to achieve the observed CME brightness.<sup>5</sup> Most of the CMEs distribution centered at 0 – 100km/s.

For slow CME, cycle 23 and 24 has been 7872 and 11190 events respectively (Figure 10).

For fast CMEs, cycle 23 and 24 has 5700 and 4284 CMEs respectively. Here, wide & fast CMEs shows similar series of distribution which shows that wide CMEs travels fast (Figure 11).

CMEs with positive and negative acceleration shows opposite power law distributions which shows that their motion is probably distributed by different mechanism (Figures 12 and 13).

### Analysis for force

Figure 14 shows distribution of force for All CMEs. CME distribution for force shows multiple peaks. Highest CME peaks occurred at  $2.00 \times 10^{13}$  N for both cycles. Predominant peak for cycle is  $2.00 \times 10^{13}$  N. Cycle 23 has a total of 12485 CMEs while cycle 24 has 17836 CMEs (Figure 14).

For cycle 23; All CMEs, normal CMEs, fast CMEs, CMEs with positive acceleration, CMEs with negative acceleration, slow CMEs, and narrow CMEs show similar trend. However, Normal CMEs, slow CMEs and CMEs with positive acceleration did not dip around year 2001 like others. Also, normal CMEs and fast CMEs did not peak in 2007 like other CMEs. Wide CMEs shows less variation and didn't quite follow the trend like others. For cycle 24; All CMEs and normal CMEs shows a more similar trend compared to others. The CME plots all seem to dip in 2018. Narrow CMEs shows a more varying normalized yearly average between the years 2011 and 2016.

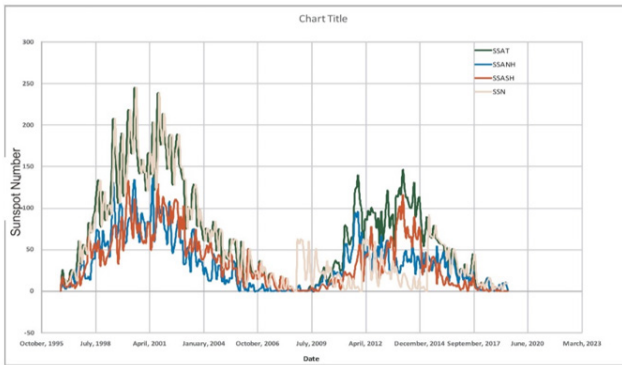


Figure 1 Monthly time series plot for SSN, SSAT, SSNH and SSASH for cycle 23 and 24.

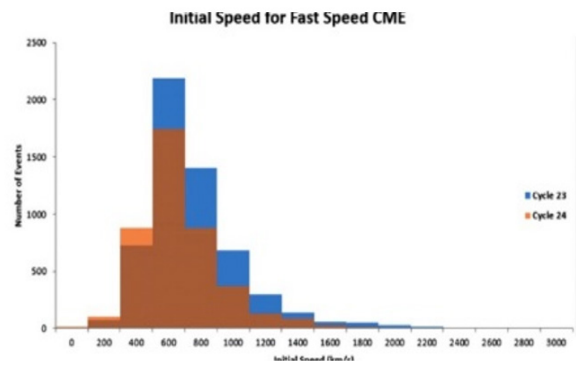


Figure 5 Distribution of Initial speed for fast CMEs.

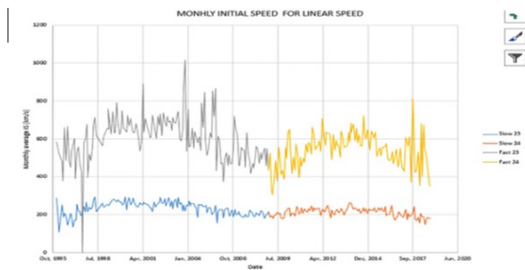


Figure 2 Monthly average time series initial speed plot for slow and fast CMEs.

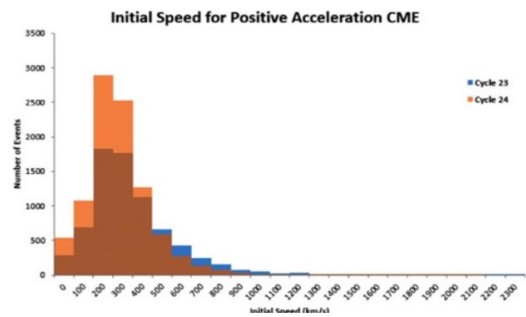


Figure 6 Distribution of Initial speed for positive acceleration CMEs.

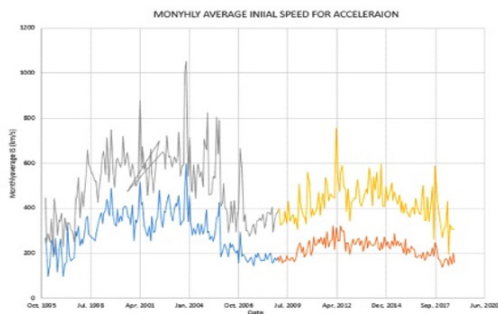


Figure 3 Monthly average time series initial speed plot for positive and negative CMEs.

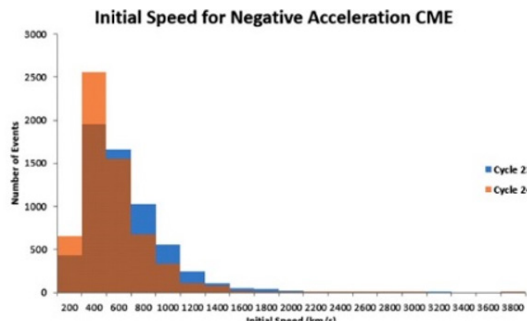


Figure 7 Distribution of Initial speed for Negative acceleration CMEs.

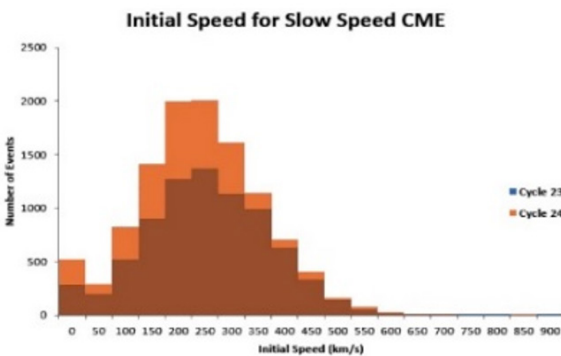


Figure 4 Distribution of Initial speed for slow CMEs.

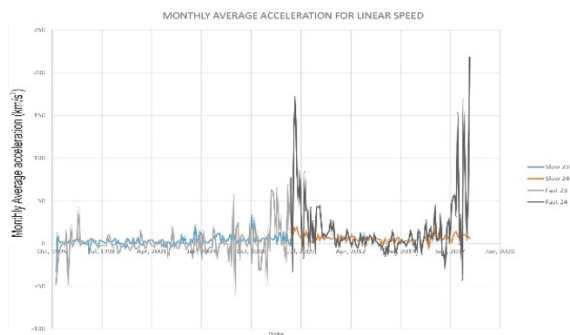


Figure 8 Monthly average time series Acceleration plot for slow and fast CMEs.

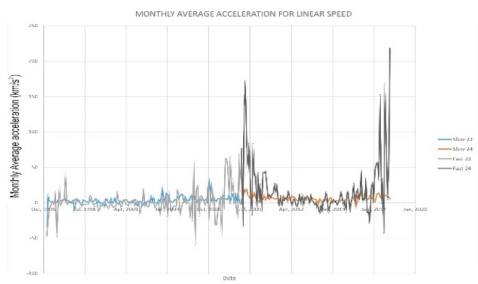


Figure 9 Monthly average time series Acceleration plot for positive and negative acceleration CMEs.

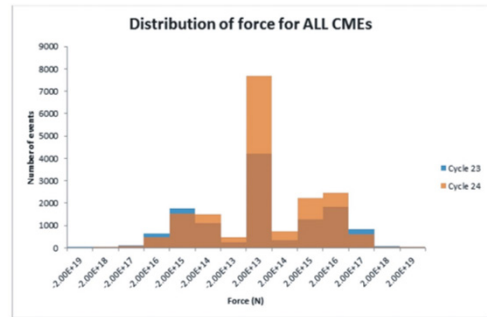


Figure 14 Distribution of force for All CMEs.

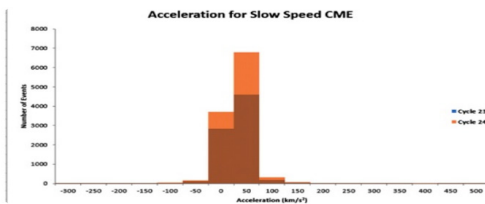


Figure 10 Distribution of acceleration for slow CMEs.

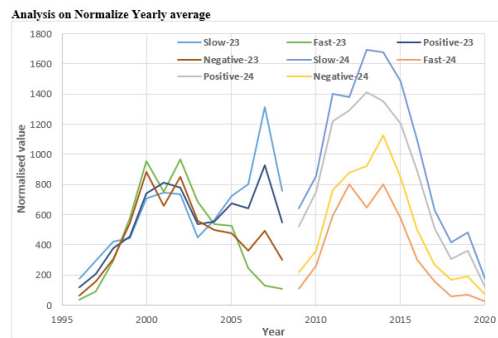


Figure 15 Normalize yearly value for ALL and segregated CMEs.

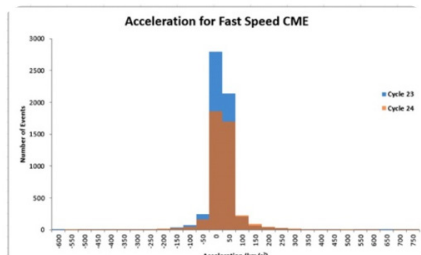


Figure 11 Distribution of acceleration for fast CMEs.

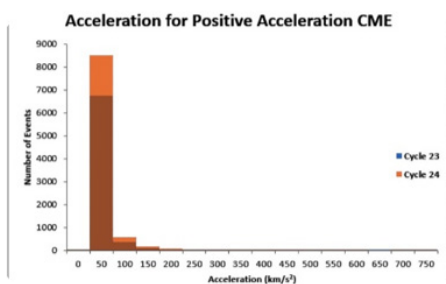


Figure 12 Distribution of acceleration for positive acceleration CMEs.

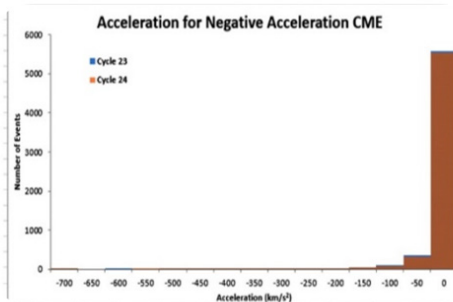


Figure 13 Distribution of acceleration for Negative acceleration CMEs.

### Summary

#### Mean value of histogram for positive acceleration

	IS	ACCEL	FORCE
CYCLE 23	346	58	2.99X1016
CYCLE 24	280	59	1.69X1016

#### Mean value of histogram for negative acceleration

	IS	ACCEL
CYCLE 23	650	-8
CYCLE 24	551	-7

#### Mean value of histogram for slow CMEs

	IS	ACCEL
CYCLE 23	250	32
CYCLE 24	241	34

#### Mean value of histogram for fast CMEs

	IS	ACCEL
CYCLE 23	760	23
CYCLE 24	680	31

- I. According to the number of Sunspots (SSNS) for solar cycle 24 has been very weak and also the least since the dawn of the space era.<sup>6</sup>
- II. For slow CMEs, initial speed decreases while acceleration increases.<sup>7</sup>
- III. For fast CMEs only acceleration parameter decreases in value from one cycle to another.<sup>8</sup>
- IV. For positive acceleration, CME parameters show decrease in initial speed and an insignificant increase in acceleration.
- V. For negative acceleration, acceleration show an almost insignificant increase while initial speed decreases.

## Conclusion

From the comparison of CME time series with solar activity parameters especially SSAT and SSN, we observe that fast CMEs follow the solar activity cycle while slow CMEs doesn't. Also negative and positive CMEs follow the solar activity cycle but lags I behind by 3 months for cycle 24. The distributions shows that slow CMEs increase in acceleration from one cycle to the other while fast CMEs shows a decrease in acceleration. There is an insignificant increase in acceleration for CMEs with positive and negative acceleration. These changes is perhaps due to effects of solar wind.

## Acknowledgements

The authors wish to thank the referee whose invaluable contributions improved the quality of this article. The CME catalog is generated and maintained by the center for solar physics and space weather, the Catholic University of America in cooperation with the Naval Research Laboratory and NASA. SOHO is a project of international cooperation between ESA and NASA.

## Conflicts of Interest

None.

## References

1. Forbes TG. A review of the genesis of Corona Mass Ejection. *JGR*. 2000;105(14):23153–23166.
2. Schween R. Space Weather: the solar perspective. *Living Rev Solar physics*. 2006;3,2.
3. Chen J, Krall J. Acceleration of Coronal Mass Ejections. *Journal of Geophysical Research*. 2003;108:1–22.
4. Georgieva K. Why the Sunspot Cycle is double peaked. *Astronomy and Astrophysics*. 2011;3–11.
5. Gopalswamy N. Climate and Weather of the sun–earth system (CAWSES): selected papers. 2007.
6. Webb DF, Howard TA. Coronal Mass Ejections: Observations. *Living Rev Solar Physics*. 2012;9:3.
7. Low BL, Zhang M. The hydromagnetic origin of the dynamical types of Solar Coronal Mass Ejections. *Astrophysical Journal letter*. 2000;504:53–56.
8. St. Cyr OC, Plunkett Michels, DJ Paswaters.